

# Quantum phase transitions with parity-symmetry breaking and hysteresis

A. Trenkwalder<sup>1</sup>, G. Spagnolli<sup>2</sup>, G. Semeghini<sup>2</sup>, S. Coop<sup>2,3</sup>, M. Landini<sup>1</sup>, P. Castilho<sup>1,4</sup>, L. Pezzè<sup>1,2,5</sup>, G. Modugno<sup>2</sup>, M. Inguscio<sup>1,2</sup>, A. Smerzi<sup>1,2,5</sup> and M. Fattori<sup>1,2\*</sup>

**Symmetry-breaking quantum phase transitions play a key role in several condensed matter, cosmology and nuclear physics theoretical models<sup>1–3</sup>. Its observation in real systems is often hampered by finite temperatures and limited control of the system parameters. In this work we report, for the first time, the experimental observation of the full quantum phase diagram across a transition where the spatial parity symmetry is broken. Our system consists of an ultracold gas with tunable attractive interactions trapped in a spatially symmetric double-well potential. At a critical value of the interaction strength, we observe a continuous quantum phase transition where the gas spontaneously localizes in one well or the other, thus breaking the underlying symmetry of the system. Furthermore, we show the robustness of the asymmetric state against controlled energy mismatch between the two wells. This is the result of hysteresis associated with an additional discontinuous quantum phase transition that we fully characterize. Our results pave the way to the study of quantum critical phenomena at finite temperature<sup>4</sup>, the investigation of macroscopic quantum tunnelling of the order parameter in the hysteretic regime and the production of strongly quantum entangled states at critical points<sup>5</sup>.**

Parity is a fundamental discrete symmetry of nature<sup>6</sup> conserved by gravitational, electromagnetic and strong interactions<sup>7</sup>. It states the invariance of a physical phenomenon under mirror reflection. Our world is pervaded by robust discrete asymmetries, spanning from the imbalance of matter and antimatter to the homo-chirality of DNA of all living organisms<sup>8</sup>. Their origin and stability is a subject of active debate. Quantum mechanics predicts that asymmetric states can be the result of phase transitions occurring at zero temperature, named in the literature as quantum phase transitions (QPTs)<sup>1,4</sup>. The breaking of a discrete symmetry via a QPT provides also asymmetric states that are particularly robust against external perturbations. Indeed, the order parameter of a continuous-symmetry-breaking QPT can freely (with no energy cost) wander along the valley of a ‘mexican hat’ Ginzburg–Landau potential (GLP) by coupling with gapless Goldstone modes<sup>9</sup>. In contrast, the order parameter of discrete-symmetry-breaking QPTs is governed by a one-dimensional double-well GLP<sup>10</sup>. The reduced dimensionality suppresses Goldstone excitations, and the order parameter can remain trapped at the bottom of one of the two wells. This provides a robust hysteresis associated with a first-order QPT.

Evidence of parity-symmetry breaking has been reported in relativistic heavy-ions collisions<sup>11</sup> and in engineered photonic

crystal fibres<sup>12</sup>. Observation of parity-symmetry breaking in a QPT has been reported for neutral atoms coupled to a high-finesse optical cavity<sup>13</sup>. However, this is a strongly dissipative system, with no direct access to the symmetry-breaking mechanism necessary to study the robustness of asymmetric states. In addition, previous theoretical studies<sup>14,15</sup> have interpreted the puzzling spectral properties of a gas of pyramidal molecules that date back to the 1950s (ref. 16), in terms of the occurrence of a QPT with parity-symmetry breaking.

In the present work we report the observation of the full phase diagram across a QPT where the spatial parity symmetry is broken. Our system consists of ultracold atoms trapped in a double-well potential<sup>17,18</sup> where the tunable strength of the attractive interparticle interaction is the control parameter of the transition. Additional control of the energy mismatch between the two wells allows driving of discontinuous first-order QPTs in the non-symmetric ordered part of the phase diagram and observation of an associated hysteretic behaviour.

In our system, the atomic ground state depends on two competing energy terms in the Hamiltonian  $H = H_a + gH_b$ , where  $H_a = \int d\mathbf{r} \Psi^\dagger(\mathbf{r})[-(\hbar^2/2m)\nabla^2 + V(\mathbf{r})]\Psi(\mathbf{r})$  includes kinetic and potential energy, and  $H_b = (2\pi\hbar^2 a_0/m) \int d\mathbf{r} \Psi^\dagger(\mathbf{r})\Psi^\dagger(\mathbf{r})\Psi(\mathbf{r})\Psi(\mathbf{r})$  accounts for contact interaction between the atoms. Here,  $\Psi(\mathbf{r})$  is the many-body wavefunction,  $\Psi^\dagger(\mathbf{r})$  its hermitian conjugate (in the following we consider normalization  $\langle \Psi^\dagger(\mathbf{r})\Psi(\mathbf{r}) \rangle = 1$ ),  $m$  the atomic mass,  $a_0$  is the Bohr radius,  $\hbar$  the reduced Planck constant and  $V(\mathbf{r})$  is a double-well trapping potential in the  $x$  direction (see Fig. 1a) and a harmonic trap in the orthogonal plane. The adimensional control parameter  $g = Na_s/a_0 < 0$  is the product of the total number of atoms  $N$  and the scattering length  $a_s < 0$  characterizing the interatomic attractive interaction. The full many-body Hamiltonian is invariant under  $x \leftrightarrow -x$  mirror reflection. This parity symmetry imposes a spatially symmetric ground state for any value of the control parameter  $g$ . Because  $H_a$  and  $H_b$  do not commute, the corresponding ground states are quite different.  $H_a$  is minimized by each atom equally spreading on both wells. A finite energy gap, specified as the tunnelling energy  $J$ , separates the ground and the first (antisymmetric) excited state of  $H_a$ .  $J$  can be tuned by controlling the height of the potential barrier between the two spatial wells. In contrast,  $gH_b$  is minimized by a linear combination of two degenerate states, one having all atoms localized in one well, the second with all atoms localized in the other well. Thanks to the competition in the Hamiltonian between the effective repulsion due to the kinetic energy and the attractive interatomic interaction, the energy gap between the two low-lying

<sup>1</sup>Istituto Nazionale di Ottica-CNR, 50019 Sesto Fiorentino, Italy. <sup>2</sup>LENS European Laboratory for Nonlinear Spectroscopy, and Dipartimento di Fisica e Astronomia, Università di Firenze, 50019 Sesto Fiorentino, Italy. <sup>3</sup>ICFO-Institut de Ciencies Fotoniques, Barcelona Institute of Science and Technology, 08860 Castelldefels (Barcelona), Spain. <sup>4</sup>Instituto de Física de São Carlos, Universidade de São Paulo, C.P. 369, 13560-970 São Carlos, São Paulo, Brazil.

<sup>5</sup>Quantum Science and Technology in Arcetri, QSTAR, 50125 Firenze, Italy. \*e-mail: fattori@lens.unifi.it

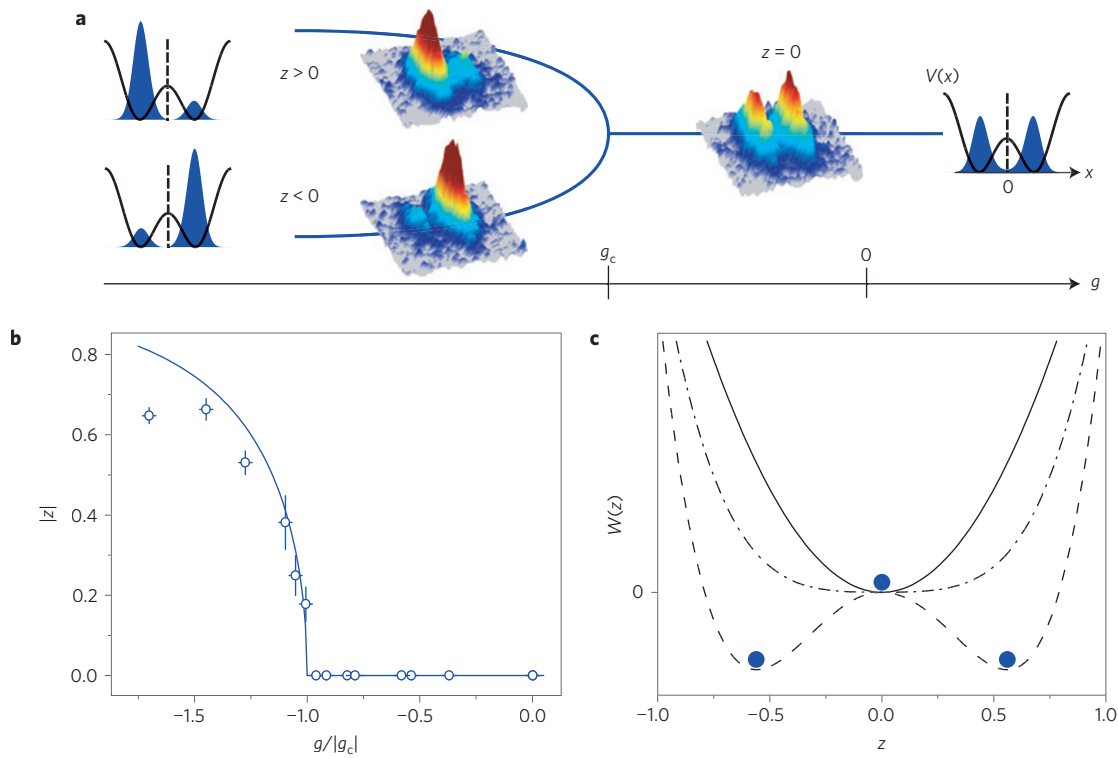


**Figure 1 | Schematics of the parity-symmetry-breaking QPT.** **a**, The ultracold atomic gas (blue wavefunction) is trapped in a double-well potential (black line). Tuning the interatomic interaction strength  $g$  to large negative values, the ground state of the system goes from a gapped symmetric state (atomic imbalance  $z = (N_L - N_R)/N = 0$ ) to two degenerate asymmetric states ( $|z| > 0$ ). The system undergoes a second-order QPT where the spatial parity symmetry, that is, reflection with respect to the vertical dotted line (symmetry axis), is broken. We show experimental absorption images in pseudo three dimensions and false colours of the atoms obtained at different values of  $g$ . **b**, Absolute value of the order parameter  $z$  as a function of the control parameter  $g$  in a balanced double well. Error bars are three times the standard deviation (see Supplementary Information). The solid line is the fitting function with  $z=0$  for  $g > g_c$  and  $z=\sqrt{1-(g_c/g)^2}$  for  $g \leq g_c$ , with  $g_c$  as fitting parameter. From a fit to the data we extract  $g_c$  with a relative uncertainty of 0.15. It agrees within 20% with the theoretical prediction. **c**, GLP  $W(z)$  for different values of  $g/|g_c|$  across the QPT:  $g/|g_c| = -0.5$ , solid line;  $g/|g_c| = -1$ , dash-dotted line;  $g/|g_c| = -1.2$ , dashed line.

states vanishes (strictly equal to zero in the thermodynamic limit  $N \rightarrow \infty$ ,  $a_s \rightarrow 0$ ) at a finite critical value of the control parameter  $g_c$ . For  $g > g_c$  the tunnelling energy  $H_a$  dominates and the system is in a symmetric configuration. For  $g \leq g_c$ , when the interaction energy  $gH_b$  prevails, the system becomes exponentially sensitive to arbitrarily small fluctuations of the energy of the two wells. This forces the majority of atoms to localize randomly in one well or the other (see Fig. 1a). The broken symmetry is characterized by a non-zero-order parameter that, in our case, is the normalized atomic population imbalance  $z = (N_L - N_R)/N$ , where  $N_L$  and  $N_R$  are the number of atoms occupying the left and the right well, respectively.

To measure  $z$  across the phase transition (see Fig. 1b) we adopt the following experimental procedure. We start by cooling a gas of  $N = 4,500$  atoms well below the Bose-Einstein condensation point until no thermal fraction can be detected (see Supplementary Information). The atoms are initially trapped in a harmonic potential, with a positive scattering length  $a_s = 3a_0$ . We reach different target values of  $g$ , above and below the critical point, by continuously transforming the harmonic trap into a double well, up to a certain barrier height and tunnelling  $J \approx 40$  Hz, and by tuning the interatomic scattering length to negative values (see Supplementary Information). When  $g > g_c$ , we find the system in a parity-symmetric disordered phase, with order parameter  $z \approx 0$  within error bars. Below the critical value, that is, for  $g < g_c$ , an ordered phase emerges with  $z$  driven away from zero. The phase transition can be theoretically described by an effective GLP

$W(z) = (\tilde{g}/2)z^2 - \sqrt{1-z^2}$ , where  $\tilde{g} = gU/J$  is the normalized control parameter and  $U$  is the bulk energy (see Supplementary Information). When  $\tilde{g}$  crosses the critical value  $\tilde{g}_c = -1$ , the shape of  $W(z)$  continuously changes from a parabola to a double well (see Fig. 1c) with minima located at  $z = \pm\sqrt{1-1/\tilde{g}^2}$  (ref. 19). The continuous variation of  $z$  indicates the occurrence of a continuous phase transition. From the experimental measurements of the order parameter we obtain a critical value  $\tilde{g}_c = -1.3 \pm 0.2$  (corresponding to a critical value of the interaction strength  $a_s = -1.8 \pm 0.3a_0$ ), in fair agreement with the theoretical prediction. The error bar is the quadratic sum of the errors coming from the fit in Fig. 1b, the atom number measurements and the estimation of the lattice depths (see Supplementary Information). We believe that the slight disagreement with respect to the expected value is mainly due to uncontrolled jumps in the value of the magnetic field whose origin has not been identified. This noise could result in a systematic shift of the interaction strength of approximately  $\pm 10\%$  (see Supplementary Information).

A one-dimensional GLP, which depends on a single real parameter, describes a phase transition with the breaking of a discrete symmetry as, for instance, the left-right symmetry in our case, or the spin-up/spin-down symmetry in the paramagnetic-to-ferromagnetic transition<sup>4</sup>. In these systems, a controlled symmetry-breaking term (in our case provided by an energy gap  $\delta$  between the two wells, see Fig. 2a) drives a first-order QPT in the ordered region of the phase diagram. This can be understood from the sudden variation of the absolute minimum of the GLP  $W(z) + \delta z$

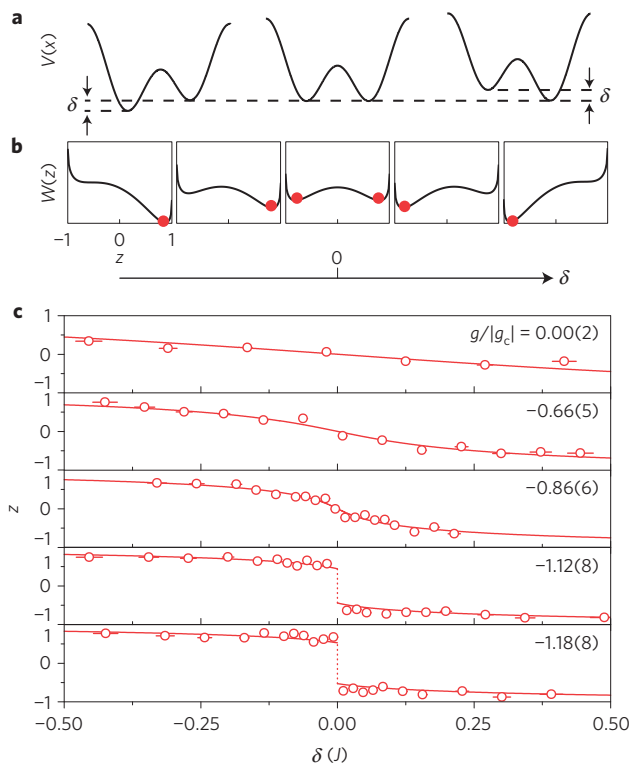


**Figure 2 | First-order QPT.** **a**, Our full control of the double-well potential include the tuning of the energy gap  $\delta$  between the two minima (see Supplementary Information). **b**, GLP  $W(z) + \delta z$ , plotted for  $g < g_c$ . Red dots represent the ground state of the system. **c**, Ground state atomic imbalance  $z$  (circles) as a function of  $\delta$ , here expressed in units of the tunnelling energy  $J$ . Different panels correspond to different values of  $g/|g_c|$ . For  $g \geq g_c$  the atomic imbalance  $z$  changes continuously as a function of  $\delta$ , whereas for  $g < g_c$  the order parameter shows a discontinuity from positive to negative values signalling the onset of a first-order phase transition. The red lines are the result of a fit using the Ginzburg–Landau theoretical model (see Supplementary Information) with  $g_c$  the only fitting parameter. Horizontal error bars come from the uncertainty in the depth of the lattices that directly affects the values of  $\delta$ . Each point has a vertical error of  $\pm 0.06$  due to limited atom detection sensitivity.

when tuning  $\delta$  from positive to negative values, as shown in Fig. 2b. We characterize this QPT by repeating the previous experimental procedure, above and below the critical point, but adding to the final potential configuration a finite and controlled value of  $\delta$ . As shown in Fig. 2c, for  $g > g_c$ , the order parameter  $z$  changes smoothly as a function of  $\delta$ , with a finite susceptibility  $\chi = |dz/d\delta|$  (measured around  $z = 0$ ). Increasing the strength of the attractive interaction causes  $z$  to depend more and more critically on  $\delta$ , and  $\chi$  diverges at the critical point (see Fig. 3). Performing the susceptibility measurements for  $g < g_c$ , we observe an abrupt jump of  $z$  when crossing the value  $\delta = 0$ , signalling the onset of the first-order phase transition (see two lowest plots in Fig. 2c). The full phase diagram showing the interplay of the observed discontinuous (first-order) and continuous (second-order) QPTs is summarized in Fig. 4a. We identify the universality class of the parity-symmetry-breaking QPT from the susceptibility measurement. A fit of  $\chi$  as a function of the interaction strength according to  $\chi = \alpha/(g - g_c)^\gamma$  is shown in Fig. 3. The two fitting parameters are  $\gamma$  and  $\alpha$ . We obtain a critical exponent  $\gamma = 1.0 \pm 0.1$ , in agreement with the Ginzburg–Landau prediction  $\gamma = 1$  (see Supplementary Information). Therefore, our QPT belongs to the universality class of the Lipkin–Meshkov–Glick model<sup>20</sup>. QPTs with the same universality class have been

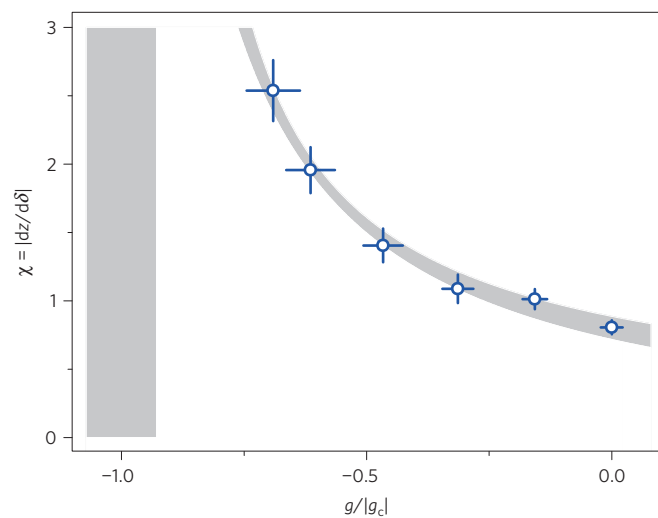


**Figure 3 | Susceptibility and measurement of the critical exponent.**

Susceptibility  $\chi = |dz/d\delta|$  of the system to potential energy gap  $\delta$  between the two wells. The measurement is performed close to the critical point for values  $g > g_c$ . The curve is a fit to the data (see text) providing a critical exponent  $-1.0 \pm 0.1$  in excellent agreement with the theoretical prediction, equal to  $-1$ . The error bar in the critical exponent comes from the indetermination of  $g_c$  (grey region).

observed in atom–cavity experiments<sup>13</sup> and spin–orbit coupled systems<sup>21–23</sup>.

Discrete-symmetry models are characterized by metastability and hysteresis when driving the system across the first-order transition. Both follow directly from the 1D nature of the effective GLP. We notice that bifurcation and hysteresis are typical phenomena in the dynamics of systems governed by a nonlinear equation of motion<sup>19,24,25</sup>. In our system, the origin of hysteresis can be understood from the shape of the GLP  $W(z) + \delta z$ , which for  $\tilde{g} < -1$  and  $|\delta| < \delta_c = [(-\tilde{g})^{2/3} - 1]^{3/2}$  shows an absolute minimum and a local minimum (see Fig. 4b and Supplementary Information). The latter corresponds to a metastable point with a lifetime depending on the macroscopic quantum tunnelling rate of the order parameter through the effective GLP. This rate is exponentially smaller than the interwell tunnelling rate of the single atoms in the double-well trap. To demonstrate hysteresis in our system, we set  $J \approx 30$  Hz, add an energy gap  $\delta_0$ , and prepare a condensate in the well with lower energy (for example the right one, with  $\delta_0 = -4J < 0$  and  $z \approx 1$ ). We then shift the relative energy of the two wells to a final value  $\delta$  in 500 ms, keeping  $J$  constant, and measure the order parameter after a short waiting time of 10 ms (green squares in Fig. 4c). The experiment is performed for different values of the control parameter  $g$ . When  $g < g_c$ , the strong attractive interaction between atoms forces the condensate to remain localized in the right well even when its energy minimum is lifted above the left well. When  $\delta$  overcomes a critical value  $\delta_c$ , a spinodal instability drives the gas down to the left towards the absolute minimum of the trapping potential in a timescale of approximately 10 ms, a fraction of  $1/J$ . An analogous behaviour is observed with an initial imbalance  $z \approx -1$  (orange circles in Fig. 4c), forming a hysteresis loop. The area of the hysteresis loop decreases with increasing  $g$ , and disappears for  $g > g_c$  (see Fig. 4c).

This work paves the way to the study of macroscopic quantum tunnelling in the hysteretic regime in the context of the quantum-to-classical transition problem<sup>26</sup>. Furthermore, it will be interesting to explore spontaneous symmetry breaking in gas mixtures as a function of the interspecies interactions<sup>27,28</sup>. Finally, our system will allow investigation of the creation of quantum

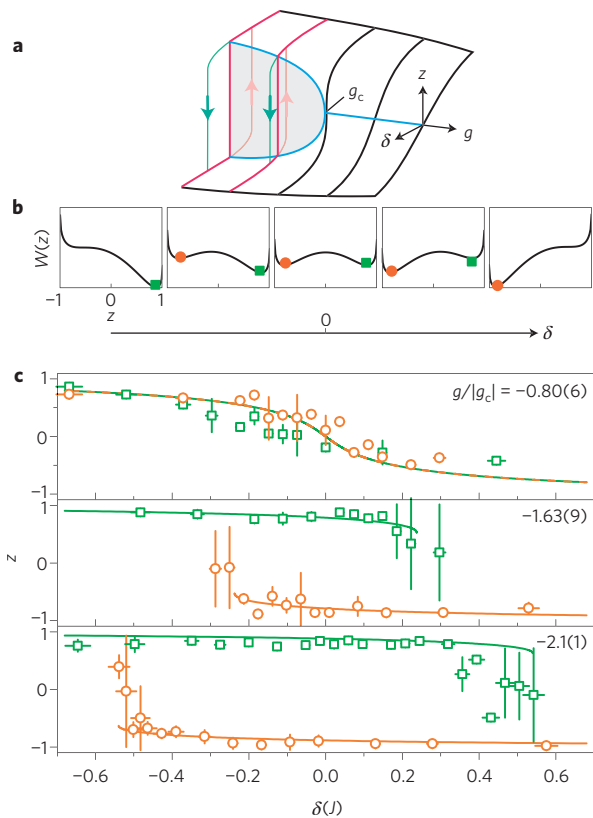


**Figure 4 | Full phase diagram and hysteresis.** **a**, Full theoretical phase diagram showing the interplay of the continuous (second-order—blue line) and discontinuous (first-order—red line) QPTs. The green and orange lines show metastable states giving access to hysteresis. **b**, GLP for  $g < g_c$  (black line) and different values of  $\delta$ . It shows absolute and local minima corresponding to ground and metastable states, respectively. Orange circles and green squares represent the states measured in **c**. **c**, Atomic imbalance as a function of the energy gap  $\delta$  between the two wells. Green squares (orange dots) are obtained cooling the gas to its ground state at negative (positive)  $\delta$  and then increasing (decreasing)  $\delta$  to the final value in 500 ms and waiting 10 ms before the measurement of the imbalance. Lines are theoretical predictions for the imbalance of the ground and the metastable states using the Ginzburg-Landau model (see Supplementary Information). Different panels correspond to different values of  $g/|g_c|$ . Large error bars signify the dynamical breaking of metastability corresponding to oscillation of the gas between the two wells.

fluctuations<sup>29</sup> and entanglement<sup>5</sup> at the critical points as a resource for precision measurements<sup>30</sup> and other quantum technologies<sup>31</sup>.

Received 2 October 2015; accepted 24 March 2016;  
published online 2 May 2016

## References

- Vojta, M. Quantum phase transitions. *Rep. Prog. Phys.* **66**, 2069–2110 (2003).
- Gegenwart, P., Si, Q. & Steglich, F. Quantum criticality in heavy-fermion metals. *Nature Phys.* **4**, 186–197 (2008).
- Giamarchi, T., Rüegg, C. & Tchernyshyov, O. Bose-Einstein condensation in magnetic insulators. *Nature Phys.* **4**, 198–204 (2008).
- Sachdev, S. *Quantum Phase Transitions* (Cambridge Univ. Press, 2001).
- Amico, L., Fazio, R., Osterloh, A. & Vedral, V. Entanglement in many-body systems. *Rev. Mod. Phys.* **80**, 517–576 (2008).
- Feynman, R. *The Character of Physical Law* (MIT Press, 1967).
- Lee, T. D. & Yang, C. N. Question of parity conservation in weak interactions. *Phys. Rev.* **104**, 254–258 (1956).
- Pasteur, L. *Oeuvres Complètes Tome I* (Masson, 1922).
- Goldstone, J., Salam, A. & Weinberg, S. Broken symmetries. *Phys. Rev.* **127**, 965–970 (1962).
- Ginzburg, V. L. & Landau, L. D. On the theory of superconductivity. *J. Exp. Theor. Phys.* **20**, 1064–1082 (1950); reprinted in *Collected Papers of L. D. Landau* 546–568 (ed. Haar, D. T.) (Gordon and Breach Science Publishers, 1965).
- Abelev, B. I. *et al.* (STAR Collaboration). Azimuthal charged-particle correlations and possible local strong parity violation. *Phys. Rev. Lett.* **103**, 251601 (2009).
- Hamel, P. *et al.* Spontaneous mirror-symmetry breaking in coupled photonic-crystal nanolasers. *Nature Photon.* **9**, 311–315 (2015).
- Baumann, K., Guerlin, C., Brennecke, F. & Esslinger, T. Dicke quantum phase transition with a superfluid gas in an optical cavity. *Nature* **464**, 1301–1306 (2010).
- Claverie, P. & Jona-Lasinio, G. Instability of tunneling and the concept of molecular structure in quantum mechanics: the case of pyramidal molecules and the enantiomer problem. *Phys. Rev. A* **33**, 2245–2253 (1986).
- Jona-Lasinio, G., Presilla, C. & Toninelli, C. Interaction induced localization in a gas of pyramidal molecules. *Phys. Rev. Lett.* **88**, 123001 (2002).
- Bleaney, B. & Loubster, J. H. Collision broadening of the ammonia inversion spectrum at high pressures. *Nature* **161**, 522–523 (1948).
- Estève, J. *et al.* Squeezing and entanglement in a Bose-Einstein condensate. *Nature* **455**, 1216–1219 (2008).
- Schumm, T. *et al.* Matter-wave interferometry in a double well on an atom chip. *Nature Phys.* **1**, 57–62 (2005).
- Raghavan, S., Smerzi, A., Fantoni, S. & Shenoy, S. R. Coherent oscillations between two weakly coupled Bose-Einstein condensates: Josephson effects,  $\pi$  oscillations, and macroscopic quantum self-trapping. *Phys. Rev. A* **59**, 620–633 (1999).
- Ulyanov, V. V. & Zaslavskii, O. B. New methods in the theory of quantum spin systems. *Phys. Rep.* **216**, 179–251 (1992).
- Lin, Y.-J., Jiménez-Garcia, K. & Spielman, I. B. Spin-orbit-coupled Bose-Einstein condensates. *Nature* **471**, 83–86 (2011).
- Zhang, J.-Y. *et al.* Collective dipole oscillations of a spin-orbit coupled Bose-Einstein condensate. *Phys. Rev. Lett.* **109**, 115301 (2012).
- Hamner, C. *et al.* Dicke-type phase transition in a spin-orbit-coupled Bose-Einstein condensate. *Nature Commun.* **5**, 4023 (2014).
- Zibold, T., Nicklas, E., Gross, C. & Oberthaler, M. K. Classical bifurcation at the transition from Rabi to Josephson dynamics. *Phys. Rev. Lett.* **105**, 204101 (2010).
- Eckel, S. *et al.* Hysteresis in a quantized superfluid atomtronic circuit. *Nature* **506**, 200–203 (2014).
- Zurek, W. H. Decoherence, einselection, and the quantum origins of the classical. *Rev. Mod. Phys.* **75**, 715–775 (2003).
- Presilla, C. & Jona-Lasinio, G. Spontaneous symmetry breaking and inversion-line spectroscopy in gas mixtures. *Phys. Rev. A* **91**, 022709 (2015).
- Relaño, A., Dukelsky, J., Pèrez-Fernández, P. & Arias, J. M. Quantum phase transitions of atom-molecule Bose mixtures in a double-well potential. *Phys. Rev. E* **90**, 042139 (2014).
- Ziń, P., Chwedeńczuk, J., Olés, B., Sacha, B. & Trippenbach, M. Critical fluctuations of an attractive Bose gas in a double-well potential. *Europhys. Lett.* **83**, 64007 (2008).
- Pezzè, L. & Smerzi, A. Entanglement, nonlinear dynamics, and the Heisenberg limit. *Phys. Rev. Lett.* **102**, 100401 (2009).
- Giovannetti, V., Lloyd, S. & Maccone, L. Quantum-enhanced measurements: beating the standard quantum limit. *Science* **306**, 1330–1336 (2004).

## Acknowledgements

We thank our colleagues of the Ultracold Quantum Gases group in Florence for constant support. We acknowledge discussions with G. Jona-Lasinio and C. Presilla. This work has been supported by ERC Starting grant AISENS, INFN (Firb RBFR08H058\_001, Micra) and by EU-FP7 (QBEC). S.C. acknowledges support from the Erasmus Mundus Doctorate Program Europhotronics (Grant No. 159224-1-2009-FR-ERA MUNDUS-EMJD) and P.C. acknowledges support from the CNPq agency of the Brazilian Ministry of Science, Technology and Innovation.

## Author contributions

A.T., G.Spagnoli and M.F. designed the experiment and performed the measurements. L.P. and A.S. worked on the theoretical model. All authors participated in the data analysis, discussion of the results and writing of the manuscript.

## Additional information

Supplementary information is available in the online version of the paper. Reprints and permissions information is available online at [www.nature.com/reprints](http://www.nature.com/reprints). Correspondence and requests for materials should be addressed to M.F.

## Competing financial interests

The authors declare no competing financial interests.